

# Transverse magnetization and torque in asymmetrical mesoscopic superconductors

Antonio R. de C. Romaguera,<sup>1,2,\*</sup> Mauro M. Doria,<sup>2,1</sup> and F. M. Peeters<sup>2</sup>

<sup>1</sup>*Instituto de Física, Universidade Federal do Rio de Janeiro, C. P. 68.528, 21941-972 Rio de Janeiro, Brazil*

<sup>2</sup>*Departement Fysica, Universiteit Antwerpen, Groenenborgerlaan 171, B-2020 Antwerpen, Belgium*

We show that asymmetrical mesoscopic superconductors bring new insight into vortex physics where we found the remarkable coexistence of long and short vortices. We study an asymmetrical mesoscopic sphere, that lacks one of its quadrants, and obtain its three-dimensional vortex patterns by solving the Ginzburg-Landau theory. We find that the vortex patterns are asymmetric whose effects are clearly visible and detectable in the transverse magnetization and torque.

PACS numbers: 74.78.Na, 74.25.Ha, 74.20.-z, 74.62.Dh

Keywords: Ginzburg-Landau theory, mesoscopic superconductor, vortex

The small volume to surface ratio in mesoscopic superconductors makes their properties distinct from the bulk materials.<sup>1</sup> For instance, in the absence of pinning and anisotropy, mesoscopic superconductors have an intrinsic magnetic hysteresis whereas bulk samples do not. Mesoscopic superconductors are intrinsically metastable since they can be in excited vortex states due to an energetic barrier upholding the decay to the groundstate.<sup>2,3</sup> Several experimental techniques have been developed to detect mesoscopic vortex states<sup>4,5,6</sup> and to reveal their new and interesting physical properties.<sup>7,8</sup> Here we obtain the transverse magnetization and torque that result from the *asymmetrical* coexistence of vortices with different lengths in mesoscopic superconductors. The general aspects of our results apply to irregularly shaped grains and, consequently, can also be relevant to the understanding of inhomogeneous bulk samples with granular structure.<sup>9,10,11</sup>

In this paper we obtain and compare the vortex patterns of two similar but distinct mesoscopic systems, namely, a *full* sphere with radius  $R = 6.0\xi$  and an asymmetrical sphere, with the same radius but lacking one of its quadrants. Hereafter we call it *minus-quarter* sphere and present here its transverse magnetization and torque. There are many reasons for the magnetic moment of a sample with volume  $V$ ,  $\boldsymbol{\mu} = V\mathbf{M}$ , not to be aligned along the applied magnetic field,  $\mathbf{H}$ . A direct measurement<sup>12,13,14</sup> of the torque

$$\boldsymbol{\tau} = \boldsymbol{\mu} \times \mathbf{H} = H\mu \sin\theta \hat{\mathbf{e}}_{\tau}, \quad (1)$$

brings insight about these distinct contributions,<sup>15,16</sup> where  $\theta$  is the angle between  $\mathbf{H}$  and  $\mathbf{M}$ . For example, vortices pinned by point-like normal inclusions (defects) are major contributors to torque due to their inability to follow a rotating applied field. This contribution is usually avoided as one seeks out true information about intrinsic properties of the superconducting state. The sample's shape and size is also another contributor and provides the basis for very high precision magnetization measurements using torque.<sup>14</sup> Basically it relies on the thin film limit, where vortices remain straight and single oriented inside the sample upon field rotation, resulting in a magnetic sign always perpendicular to the major

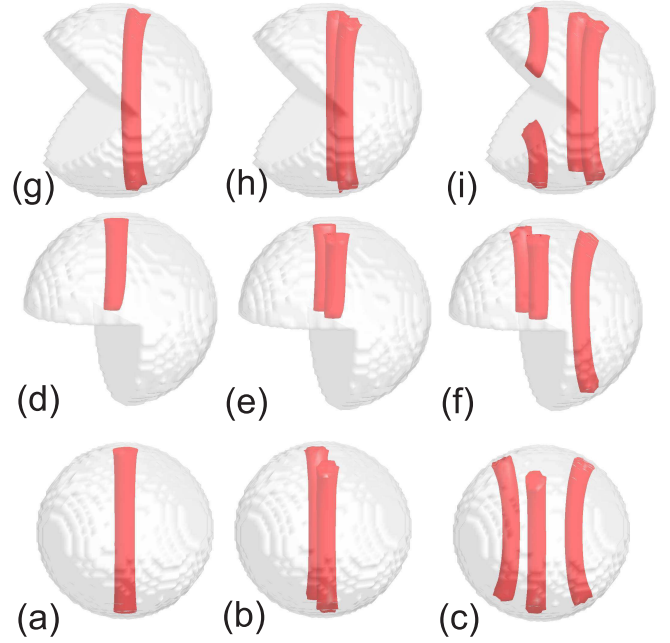


FIG. 1: (Color online) Three-dimensional iso-density plots taken at 20% of the maximum density  $|\psi|^2$ . Each iso-contour is a single surface made of the vortices and the superconductor surface. The magnetic field is directed from bottom-to-top with  $H/H_{c2} = 0.16$  (a), 0.29 (b), 0.35 (c), 0.27 (d), 0.39 (e), 0.49 (f), 0.35 (g), 0.48 (h), and 0.54 (i). The figures correspond to the *full* sphere (a)-(c) and to the *minus-quarter* sphere, positioned in two ways, ((d)-(f) and (g)-(i), with respect to the field.

surfaces. The general misalignment between the applied field and the sample's major axis produces a torque, even for a regularly shaped superconductor. Hence to obtain a torque it suffices that the circulating supercurrent yields a magnetic field response not oriented along the applied field that gave rise to it. Asymmetry leads to such effect and we show here that it provides a useful tool to probe the physics of mesoscopic superconductors.

In this paper we provide the first study of a mesoscopic superconductor with a transverse ( $M_x$ ) magnetization, thanks to the use of a truly three-dimensional

approach.<sup>17,18</sup> The found effects in the transverse magnetization and in the torque are within reach of present experimental detection.<sup>14</sup> For instance, a coherence length of  $\xi \simeq 100$  nm leads to  $H_{c2} = \Phi_0/2\pi\xi^2 \simeq 300$  Gauss.<sup>19</sup> If the penetration length is comparable to the sphere's radius  $R = 0.6 \mu\text{m}$ , then the transverse magnetization is approximately ten times smaller,  $M_x \simeq 10^{-3}H_{c2} \simeq 0,3$  Gauss than the longitudinal one  $M_z \simeq 10^{-2}H_{c2} \simeq 3$  Gauss. The magnetic moment of this sphere is  $\mu \sim M_z V \simeq 7.0 \times 10^{-12}$  emu ( $V = 72\pi\xi^3 \simeq 7.63 \times 10^{-13}$  cm<sup>3</sup> for the *minus-quarter* sphere). The torque,  $\tau_y = -M_x H_z V \simeq 10^{-3}H_{c2}^2 V$  becomes  $\tau_y = 4.0 \times 10^{-12}$  erg.

Fig. 1 summarizes the novel aspects brought by asymmetry showing the Cooper pair density,  $|\psi(\mathbf{r})|^2$ , obtained from our numerical simulations for selected values and orientations of the applied field. States with at most three vortices were selected to help to understand the basic effects caused by asymmetry. For all cases the magnetic field is oriented along the bottom-to-top direction. In those mesoscopic systems vortices are naturally curved<sup>20</sup> because the entrance and exit of the vortex lines must be perpendicular to the surface,<sup>21</sup> a fact that causes a closely packed configuration near to the equatorial region, as previously found.<sup>17</sup>

Fig. 1(d) best represents the effects of the asymme-

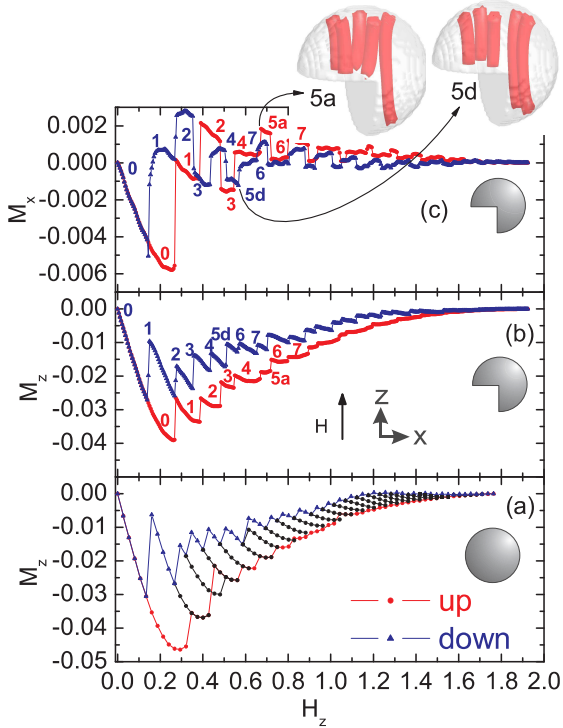


FIG. 2: (Color online) The magnetization for a full field cycle is shown here, (a) for the *full* and (b)-(c) for the *minus-quarter* sphere. The ascending (red) and descending (blue) branches are labeled for the first nine vortex states. Selected iso-plots obtained in ascending and descending fields show the degeneracy of the 5 state. The full non-intersecting magnetization branches are shown just for the *full* sphere.

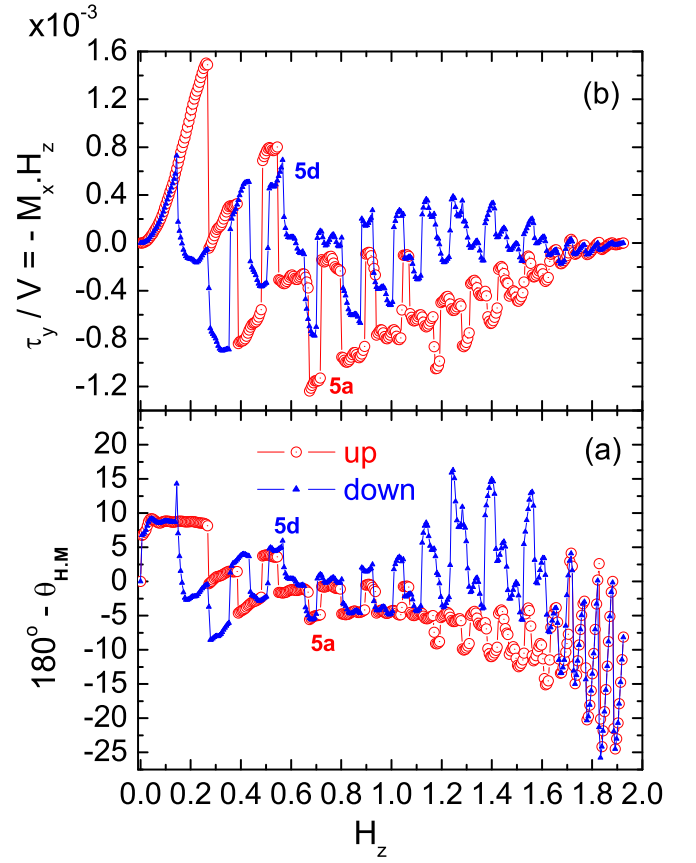


FIG. 3: (Color online) The ascending (red) and descending (blue) torque branches are shown here in (a) sub-plot and the corresponding misalignment angle in (b) sub-plot.

try where the position of the short vortex very close to the center of the *minus-quarter* sphere is determined by: (i) the spherical shell pushing the vortex near the central axis where the shielding current offers maximal stability<sup>22</sup> and, (ii) the flat surface of the missing quadrant where the vortex length is half of the one for a full sphere. As a consequence, the vortex is displaced from the central axis, breaking the rotational symmetry in the northern hemisphere resulting in transverse magnetization and torque. The second vortex has the same faith of the first one, it is also a short vortex that gets as close as possible to the central axis (Fig. 1(e)). The situation changes for the third vortex, possibly because  $R = 6.0\xi$  is just too small to accommodate it in the quadrant, forcing its nucleation in the full hemisphere where it becomes the first long vortex. Asymmetry brings peculiar, not always intuitive, features. For instance the rotation of the *minus-quarter* sphere by  $45^\circ$  leads to new vortex configurations not accessible in case of the previous alignment. Now the long vortices nucleate first and short vortices enter in pairs afterwards, as shown in Figs. 1(g)-(i), with increasing field. In summary asymmetry brings new situations that can bring further information about vortex patterns in mesoscopic superconductor. They are de-

tectable in the transverse magnetization and the torque, bringing inside information about vortex patterns in such systems.

The Ginzburg-Landau theory, derived near the critical temperature, is applicable at much lower temperatures for the mesoscopic superconductors, where it was found to give a fair description of its magnetic properties.<sup>4,19</sup> We solve the full three-dimensional Ginzburg-Landau theory for the asymmetrical superconductor by the numerical procedure described in Refs. 17,23, that minimizes the free energy with the boundary conditions included. In this approach the superconductor shape is characterized by a step-like function in the free energy (1 inside the superconductor and 0 outside). Here we also include an intermediate step inside the superconductor (0.8 within a layer of thickness  $0.5\xi$ ) to stabilize the states for fields near  $H_{c3}$ , according to Ref. 17. The present results are under the approximation that the applied field uniformly permeates the mesoscopic superconductor so that the magnetic shielding is safely ignored. A discretized gauge invariant version of the Ginzburg-Landau free energy is minimized in a cubic mesh with  $46 \times 46 \times 46$  points<sup>17</sup> and the magnetization is directly determined from  $\mathbf{M} = \text{const} (1/2c) \int \mathbf{r} \times \mathbf{J} dv/V$ , where  $\mathbf{J}$  is the supercurrent in the mesoscopic superconductor volume and *const* a free parameter associated to the demagnetization tensor<sup>24,25</sup>  $\mathbf{D}$ , and so, obtained in our numerical simulations from the zero vortex branch (Meissner phase) at small  $H$ :  $\mathbf{H} + 4\pi\mathbf{D} \cdot \mathbf{M} = 0$ . We apply the inverted relations  $M_x = (-D_{zz}H_x + D_{xz}H_z)/\det$  and  $M_z = (D_{zx}H_x - D_{xx}H_z)/\det$  with  $\det = D_{zz}D_{xx} - D_{xz}D_{zx}$  in our numerical analysis to find that for the *full* sphere the demagnetization tensor reduces to a single scalar,  $D$ , as expected, which is adjusted to the well known value<sup>24,25</sup> of  $D = 1/3$  and for the *minus-quarter* sphere  $D_{xx} = D_{zz}$ ,  $D_{xz} = D_{zx}$ , and also that  $D_{zz}/D = 1.20$  and  $D_{zx}/D = -0.184$ . In the rest of the paper we use the gaussian system of units and express both the magnetization and the applied field in terms of  $H_{c2}$ , the bulk upper critical field, and the torque per volume in units of  $H_{c2}^2$ .

Fig. 2 shows the magnetization of the *full* and the *minus-quarter* spheres. We use the notation *long+short*  $\rightarrow$  (*long*, *short*) to express the *minus-quarter* sphere states, whose first nine ones, labeled in Figs. 2(b) and (c), are given by:  $0 \rightarrow (0,0)$ ,  $1 \rightarrow (0,1)$ ,  $2 \rightarrow (0,2)$ ,  $3 \rightarrow (1,2)$ ,  $4 \rightarrow (1,3)$ ,  $5d \rightarrow (1,4)$ ,  $5a \rightarrow (2,3)$ ,  $6 \rightarrow (2,4)$ , and  $7 \rightarrow (2,5)$ . Notice that there are two 5 vortex states,  $5a$ , and  $5d$ , the first being the lowest in energy, and therefore reached by the ascending field. These two states can coexist under the same field although Fig. 2 does not show the corresponding prolongation of the  $5a$  and  $5d$  curves. This degeneracy is a new and interesting aspect brought by asymmetry which shows that the total number of vortices not always determines iniquely the magnetization branch. We found 24 states for the *full* spheres and at least 26 for the *minus-quarter* sphere. The higher vortex states, which live near to the normal state,

become increasingly difficult to identify and so, required more precision than considered here. The magnetization curves were obtained to a full cycle field sweep that starts at zero, reaches the maximum possible value ( $H_{c3}$ ) (ascending branch, red color), and finally is lowered back to zero (descending branch, blue color). Figs. 2(a) and (b) show the magnetization component along the field,  $M_z$ , with the expected feature of rounded branches for ascending field and of a tooth-saw structure for descending field. This behavior has been extensively discussed both theoretically<sup>26,27,28</sup> and also experimentally.<sup>4</sup> The full stability region for the different vortex configuration is only displayed here for the *full* sphere (Fig. 2(a)). Its construction requires numerous sweeps starting at intermediate applied field values. Notice the distinct features of  $M_x$  in comparison to the  $M_z$ . The ascending and descending branches are entangled and have an underlying structure that approximately breaks in distinct families, associated to odd and even number of vortices. These branches display a wiggled structure due to vortex repositioning that cause abrupt changes in vortex length, and so in energy and in current flow.

The vortex entrance or exit can be detected through the transverse magnetization, whose sign changes accordingly, as seen in Fig. 2(c). Mesoscopic superconductors are known to be able to exhibit a paramagnetic signal when in a metastable vortex state<sup>29,30</sup> but this is not the case for the sphere, as the dominant component ( $M_z$ ) remains steadily oppositely oriented to the applied field. However a change of sign in  $M_x$  implies that the torque flips direction, as shown in Fig. 3. Moreover the torque is proportional to the applied field and it gets naturally enhanced in the regime between  $H_{c2}$  and  $H_{c3}$ ,

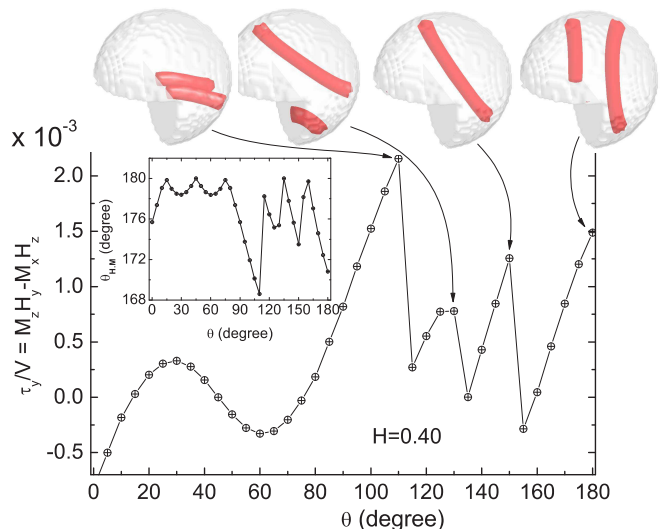


FIG. 4: (Color online) The torque is shown upon rotation of the fixed applied field ( $H = 0.40$ ) in  $5^\circ$  increments. The inset shows the angle between  $\mathbf{M}$  and  $\mathbf{H}$  versus the applied field angle. Selected iso-plot configurations for  $110^\circ$ ,  $130^\circ$ ,  $150^\circ$ , and  $180^\circ$  are also displayed here.

contrary to the magnetization, which gets dim in this region. The magnetization angle,  $180^\circ - \theta$ , shows that the misalignment with the applied field is about  $10^\circ$  for small fields and it oscillates above  $H_{c2}$ . Thus, torque measurement can be very helpful in the detection of high vortex states where the onset of a vortex configuration causes an abrupt change of sign. As an example, Fig. 4 shows the torque for a rotating field of intensity  $H = 0.4$ . The selected initial configuration for  $0^\circ$  is the ground state for this field, made of two short vortices (see Fig. 1(e)). As the field rotates by an angular increments of  $5^\circ$ , the two short vortices follow along and this configuration remains stable until  $110^\circ$ , albeit the fact that during this process the torque flips sign four times! The torque suffers an abrupt drop at  $115^\circ$  signaling the entrance of a new vortex pattern. One of the short vortices is replaced by a long vortex and the remaining short vortex moves to the center of the *minus-quarter* sphere. This long and short vortex configuration, i.e. (1, 1) lasts until the next torque transition at  $130^\circ$ , where a single long vortex becomes the

accessed configuration (from  $135^\circ$  until  $150^\circ$ ). Thus the Fig. 1(g) state is reached in this way. The last abrupt drop brings back the (1, 1) configuration from  $155^\circ$  until  $180^\circ$ . The final state does not coincide with the initial one, and is not included as one of the available stable configurations listed in Fig. 1. Thus it is a very high excited state much above the ground state. Nevertheless it became accessible by virtue of the torque.

In conclusion we have shown here that the extra complexity of vortex patterns in asymmetrical mesoscopic superconductors, under a tilted field, can be used as a tool for vortex detection through the measurement of the transverse magnetization and the torque.

A. R. de C. Romaguera acknowledges the Brazilian agency CNPq for financial support. M. M. Doria thanks CNPq, FAPERJ, Instituto do Milênio de Nanotecnologia (Brazil) and BOF/UA (Belgium). F. M. Peeters acknowledges support from the Flemish Science Foundation (FWO-VI), the Belgian Science Policy (IUAP) and the ESF-AQDJJ network.

- 
- \* Electronic address: ton@if.ufrj.br
- <sup>1</sup> A. T. Dorsey, Nature (London) **408**, 783 (2000).
  - <sup>2</sup> B. J. Baelus, F. M. Peeters, and V. A. Schweigert, Phys. Rev. B **63**, 144517 (2001).
  - <sup>3</sup> P. S. Deo, V. A. Schweigert, and F. M. Peeters, Phys. Rev. B **59**, 6039 (1999).
  - <sup>4</sup> A. K. Geim, I. V. Grigorieva, S. V. Dubonos, J. G. S. Lok, J. C. Maan, A. E. Filippov, and F. M. Peeters, Nature (London) **390**, 259 (1997).
  - <sup>5</sup> C. A. Bolle, V. Aksyuk, F. Pardo, P. L. Gammel, E. Zeldov, E. Bucher, R. Boie, D. J. Bishop, and D. R. Nelson, Nature (London) **399**, 43 (1999).
  - <sup>6</sup> A. K. Geim, S. V. Dubonos, J. J. Palacios, I. V. Grigorieva, M. Henini, and J. J. Schermer, Phys. Rev. Lett. **85**, 1528 (2000).
  - <sup>7</sup> I. V. Grigorieva, W. Escoffier, J. Richardson, L. Y. Vinnikov, S. Dubonos, and V. Oboznov, Phys. Rev. Lett. **96**, 077005 (2006).
  - <sup>8</sup> A. Kanda, B. J. Baelus, F. M. Peeters, K. Kadowaki, and Y. Ootuka, Phys. Rev. Lett. **93**, 257002 (2004).
  - <sup>9</sup> A. R. Jurelo, J. V. Kunzler, J. Schaf, P. Pureur, and J. Rosenblatt, Phys. Rev. B **56**, 14815 (1997).
  - <sup>10</sup> C. Howald, P. Fournier, and A. Kapitulnik, Phys. Rev. B **64**, 100504 (2001).
  - <sup>11</sup> T. Ekino et al, Physica C **426-431**, 230 (2005).
  - <sup>12</sup> M. M. Doria and I. G. de Oliveira, Phys. Rev. B **49**, 6205 (1994).
  - <sup>13</sup> V. G. Kogan, Phys. Rev. Lett. **89**, 237005 (2002).
  - <sup>14</sup> Y. Wang, L. Li, M. J. Naughton, G. D. Gu, S. Uchida, and N. P. Ong, Phys. Rev. Lett. **95**, 247002 (2005).
  - <sup>15</sup> D. E. Farrell, C. M. Williams, S. A. Wolf, N. P. Bansal, and V. G. Kogan, Phys. Rev. Lett. **61**, 2805 (1988).
  - <sup>16</sup> H. Won and K. Maki, Europhys. Lett. **34**, 453 (1996).
  - <sup>17</sup> M. M. Doria, A. R. de C. Romaguera, and F. M. Peeters, Phys. Rev. B **75**, 064505 (2007).
  - <sup>18</sup> A. R. de C. Romaguera, M. M. Doria, and F. M. Peeters, cond-mat/0609576 (2006).
  - <sup>19</sup> P. S. Deo, V. A. Schweigert, F. M. Peeters, and A. K. Geim, Phys. Rev. Lett. **79**, 4653 (1997).
  - <sup>20</sup> A. R. de C. Romaguera, M. M. Doria, and F. M. Peeters, Phys. Rev. B **In press** (2007).
  - <sup>21</sup> E. H. Brandt, J. Low Temp. Phys. **42**, 557 (1981).
  - <sup>22</sup> B. J. Baelus, D. Sun, and F. M. Peeters, Phys. Rev. B **In press** (2007).
  - <sup>23</sup> M. M. Doria and A. R. de C. Romaguera, Europhys. Lett. **67**, 446 (2004).
  - <sup>24</sup> J. A. Osborn, Phys. Rev. **67**, 351 (1945).
  - <sup>25</sup> M. Beleggia, M. D. Graef, and Y. T. Millev, J. Phys. D: Appl. Phys. **39**, 891 (2006).
  - <sup>26</sup> V. A. Schweigert, F. M. Peeters, and P. S. Deo, Phys. Rev. Lett. **81**, 2783 (1998).
  - <sup>27</sup> V. A. Schweigert and F. M. Peeters, Phys. Rev. Lett. **83**, 2409 (1999).
  - <sup>28</sup> B. J. Baelus and F. M. Peeters, Phys. Rev. B **65**, 104515 (2002).
  - <sup>29</sup> J. J. Palacios, Phys. Rev. Lett. **84**, 1796 (2000).
  - <sup>30</sup> A. K. Geim, S. V. Dubonos, J. G. S. Lok, M. Henini, and J. C. Maan, Nature (London) **396**, 144 (1998).